Vlasov-Maxwell kinetic simulations of radio-frequency-driven ion flows in magnetized plasmas

Chiara Marchetto
Istituto di Fisica del Plasma, CNR, EURATOM-ENEA-CNR Association, Milan, Italy;
Dipartimento di Ingegneria Nucleare, Politecnico di Milano, Milano, Italy;
and Istituto Nazionale di Fisica della Materia, Universita' di Milano, Milano, Italy

Francesco Califano
Istituto di Fisica del Plasma, CNR, EURATOM-ENEA-CNR Association, Milan, Italy
and Istituto Nazionale di Fisica della Materia, Universita' di Pisa, Pisa, Italy

Maurizio Lontano
Istituto di Fisica del Plasma, CNR, EURATOM-ENEA-CNR Association, Milan, Italy
(Received 28 March 2002; published 7 February 2003)

The generation of a coherent ion flow due to the injection in a plasma of a purely electrostatic wave of finite amplitude, propagating at right angle with the ambient uniform magnetic field, is investigated making use of a kinetic code which solves the fully nonlinear Vlasov equations for electrons and ions, coupled with the Maxwell equations, in one spatial and two velocity dimensions. A uniformly magnetized slab plasma is considered. The wave frequency is assumed in the range of the fourth harmonic of the ion cyclotron frequency, and the wave vector is chosen in order to model the propagation of an ion Bernstein wave. The computation of the first-order moment of the ion distribution function shows that indeed a quasistationary transverse average ion drift velocity is produced. The time evolution of the ion distribution function undergoes a ''resonant'' interaction of Cherenkov type, even if the plasma ions are magnetized ($\omega_{ci}/\omega_{pi} \approx 0.5$). During the wave-plasma interaction, the electron distribution function remains Gaussian-like, while increasing its energy content.

DOI: 10.1103/PhysRevE.67.026405 PACS number(s): 52.35.Mw, 52.35.Hr, 52.50.Qt, 52.35.Ra

I. INTRODUCTION

In the past years, it has been predicted by several theoretical studies [1–4] that the ion Bernstein waves (IBWs), which are compressional electrostatic waves in hot magnetized plasmas can be effectively used to generate sheared poloidal flows in a tokamak plasma. The wave-plasma interaction would produce localized ''transport barriers,'' which reduce the energy leakage from the plasma core towards its periphery. The physical mechanism through which IBWs influence the energy transport in a plasma relies on the generation of a poloidal ion flow with a radial gradient, around the spatial region where high absorption is expected (the fourth ion cyclotron harmonic in the tokamak FTU [5]), thus shortening the correlation length of the turbulent fluctuations [6]. Few experiments, where IBWs have been excited by exploiting the conversion of an electron plasma wave at the lower hybrid resonant layer, in a high temperature plasma, have shown the effective occurrence of poloidal sheared flows [7,8] and the enhanced confinement properties of the target plasma [5,9].

According to the present understanding, the ion flow generation can be ascribed to the radio-frequency induced kinetic pressure [2], and to the direct momentum input from the wave to the resonant absorbing ions. The present analysis is aimed to elucidate the intimate nature of the latter mechanism, which can be better controlled from the outside due to the effective absorption of IBWs in a hot plasma and to the expected good radial localization.

The motion of a charged particle in the presence of a constant magnetic field and under the action of a perpendicularly propagating purely electrostatic wave has been studied in Refs. [10–16] for different purposes. In Refs. [10–13], the frequency of the pump was taken in the lower hybrid range, in regimes where it is several times higher than the ion cyclotron frequency ($\omega_0 \approx 30\omega_{ci}$). There, independent of how close the frequency was to a high-order ion cyclotron harmonic, a stochastic regime of interaction was observed. This early analysis differs in what we are presenting in this paper, due to our interest in the ion response to a pump wave with a much lower frequency, in particular, close to one of the first cyclotron harmonics (the fourth one in the specific case here considered).

The problem was tackled also in connection with the so-called ''Bernstein-Landau paradox'' [14,15]. In this context, the following fully nonlinear investigation shows that, at frequencies of few cyclotron harmonics, the wave absorption of a purely normal electrostatic wave takes place via the Cherenkov mechanism.

More recently, an analytical investigation based on the study of the single particle trajectories of the ions in the presence of a strong uniform magnetic field, under the action of a monochromatic propagating electrostatic wave with frequency of the order of the fourth ion cyclotron harmonic, has been performed [16]. It has been shown that the transverse (both to the wave propagation and to the magnetic field directions) ion average velocity is produced by the Lorentz force in the form of a particle drift at the second order in the wave amplitude. An essential ingredient is to correctly describe the nonlinearity in the particle trajectory, due to the propagating electric field, which is at the origin of the ion drift. These results are obtained in the frame of an expansion

of the motion equation for small amplitude; this assumption can be quite limiting for IBWs which can develop strong electric fields due to their low group velocity.

In the present paper, we investigate the interaction of a given, purely longitudinal, propagating wave with a magnetized electron-ion plasma, by means of a kinetic Vlasov-Maxwell numerical code [17,18]. The aim of our study is to elucidate the nature of the generation of an average transverse ion velocity due to the action of the externally driven wave. The IBW is modeled by the pump wave which is characterized by a frequency in the range of the fourth harmonic of the ion cyclotron frequency, and by a wavelength of the order of the Larmor radius of a thermal ion. The electrostatic pump wave is not treated self-consistently. Its amplitude, frequency, and wave vector are external parameters, which do not evolve during the integration. The self-consistently generated electrostatic field is found to be of the order of 20% of the pump amplitude. The hydrodynamic and kinetic aspects of the wave-plasma interaction are discussed with reference to the regime of interaction in the IBW experiment in FTU [5]. Due to the basic character of our study and since we are dealing with typical IBW-FTU parameters, we have chosen to explore the plasma response to several pump frequencies, without varying other parameter values, instead of following the exact linear dispersion relation.

Recently, kinetic Vlasov simulations have revealed themselves as a unique tool to investigate the microscopic and the macroscopic aspects of the interaction of propagating and standing longitudinal waves in a multicomponent plasma [19–21]. In particular, several nonlinear processes such as wave breaking, particle trapping, anomalous heating, particle acceleration, and ponderomotive effects, which are related to the finite amplitude of the pump field, are consistently described in a kinetic framework. In this paper, we apply such a powerful method of investigation to the case of a magnetized electron-ion plasma.

In Sec. II the physical model is presented. In Sec. III the time evolution of the macroscopic physical quantities is discussed and the generation of an average transverse ion flow is shown. Section IV is devoted to the description of the electron and ion distribution functions. An extended discussion of the results is contained in Sec. V. Finally, in Sec. VI the main physical achievements of the work and some problems still to be investigated are summarized.

II. THE KINETIC MODEL

The present analysis is based on the numerical integration of Vlasov-Maxwell system of equations for a two-component plasma immersed in an externally applied uniform magnetic field ($\mathbf{B}_0 = B_0 \mathbf{e}_z$) under the action of a pump longitudinal wave propagating perpendicularly to it (its wave vector being $\mathbf{k} = k\mathbf{e}_x$). The system of equations, written in dimensionless variables, reads

$$\frac{\partial f_a}{\partial t} + v_x \frac{\partial f_a}{\partial x} - \Lambda_a \left\{ [E_x(x,t) + E_{dr}(x,t) + B_z v_y] \frac{\partial f_a}{\partial v_x} + [E_y - B_z v_x] \frac{\partial f_a}{\partial v_y} \right\} = 0, \tag{1}$$

$$\frac{\partial E_x}{\partial x} = \int\int dv_x dv_y f_i(x,v_x,v_y,t) - \int\int dv_x dv_y f_e(x,v_x,v_y,t), \tag{2}$$

$$\frac{\partial E_y}{\partial x} = -\frac{\partial B_z}{\partial t}, \tag{3}$$

$$\frac{\partial B_z}{\partial x} = -\frac{\partial E_y}{\partial t} - \int\int dv_x dv_y v_y f_i(x,v_x,v_y,t) + \int\int dv_x dv_y v_y f_e(x,v_x,v_y,t). \tag{4}$$

Moreover, the (normalized) propagating electrostatic field $E_{dr}(x,t) = a \sin(\omega_0 t - k_0 x)$ is applied to the system throughout the interaction time. In the above equations, the following normalization rules have been adopted: $\omega_{pi} t \to t$, $\mathbf{v}/c \to \mathbf{v}$, $\omega_{pi} x/c \to x$, $f_a c^2/n_{0a} \to f_a$, $eE(B)/m_i c \omega_{pi} \to E(B)$. At $t=0$, the electron and ion distribution functions are Maxwellian, i.e., $f_\alpha(t=0) = \pi^{-1/2} \exp(-v^2/\beta_\alpha)$, where $\beta_\alpha = v_{t\alpha}^2/c^2$. Since we are integrating both the electron and the ion Vlasov equations, very different time and spatial scales are dealt with leading to a considerable computational time. In order to maintain it within reasonable limits, a reduced ion-to-electron mass ratio of 50 has been assumed throughout the present investigation, which accounts for the values of $\Lambda_i = -1$ and $\Lambda_e = 50$. Moreover, q_α, m_α, T_α, and $v_{t\alpha} = (2T_\alpha/m_\alpha)^{1/2}$ are the electric charge, the mass, the temperature, and the thermal velocity of the α species, respectively, c is the vacuum speed of light, e is the modulus of the electron charge. Equations (1)–(4) have been numerically integrated with periodic boundary conditions in the spatial interval $x \in [0, 3\lambda_0]$, where $\lambda_0 = 2\pi/k_0 = 1.8 \times 10^{-2}$ is the normalized pump wavelength. Here, $k_0 \approx 349$. At $t=0$, both electrons and ions are at the equilibrium and no electromagnetic field is present. The analysis has been performed for the pump frequency varying around the fourth ion cyclotron harmonic, i.e., $\omega_0 \approx 4\omega_{ci}$, and the pump wavelength λ_0 of the order of the ion Larmor radius, i.e., $k_0 \rho_{Li} > 1$, where $\rho_{Li} = v_{ti}/\omega_{ci}$. The reference parameter values (at $t=0$) are those characterizing the IBW-FTU experiment [22]: $n_e = n_i = 5 \times 10^{13}$ cm^{-3}, $T_e = T_i = 1$ keV, $B_0 = 7.8$ T, for the plasma, and $2\pi/\omega_0 = 4 f_{ci} \approx 433$ MHz (where $f_{ci} = 2\pi/\omega_{ci} = eB_0/m_i c$), $N_\perp = 1000$ (IBW refractive index), $\hat{E}_{dr} \approx 1$ kV/cm (the peak electric field value of the excited IBW), for the wave. A suitable rescaling of the ion parameter values is needed in order to treat the reduced value of the ion mass.

The chosen values correspond to quiver parameters

$$\frac{\tilde{v}_e}{v_{te}} \approx 3.4 \times 10^{-1}, \quad \frac{\tilde{v}_i}{v_{ti}} \approx 8 \times 10^{-3} \frac{Z}{\sqrt{A}},$$

for electrons and ions, respectively, where $\tilde{v}_\alpha = q_\alpha \hat{E}_{dr}/m_\alpha \omega_0$ is the *quiver velocity* of the particle of spe-

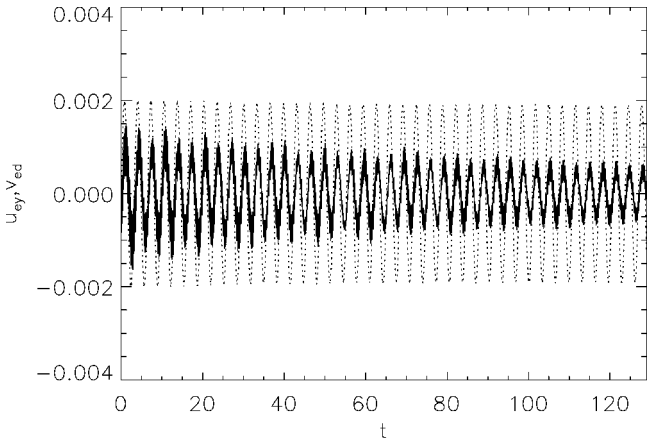

FIG. 1. U_{ey} (solid line) and $v_{ed}=-E_x/B_z$ (dotted line) are shown versus time at $x=0.038$, for $\omega_0=1.93$, and $a=10^{-3}$.

cies α in the oscillating electric field of peak amplitude $\hat{E}_{dr}$ and angular frequency ω_0. Here, the charge state Z and the mass number A of the ions have been introduced. On the basis of such estimates, an almost linear ion dynamics is expected, while electrons could manifest a non linear response to the applied field. As we shall see in the following sections, the picture is more complicated in that the kinetics of the interaction will lead to a strongly nonlinear coupling between the wave and the ions.

III. THE FLUID PLASMA RESPONSE

In the present section, the time evolution of the normalized fluid quantities associated with the electron-ion fluid is discussed. In particular, we shall speak in terms of the *number density*

$$n_\alpha(x,t)=\int_{-\infty}^{+\infty}dv_x\int_{-\infty}^{+\infty}dv_y f_\alpha(x,v_x,v_y,t), \tag{5}$$

of the *fluid velocity*

$$\mathbf{U}_\alpha(x,t)=\frac{1}{n_\alpha}\int_{-\infty}^{+\infty}dv_x\int_{-\infty}^{+\infty}dv_y\mathbf{v}f_\alpha(x,v_x,v_y,t), \tag{6}$$

and of the *temperature*, or average internal energy

$$T_\alpha(x,t)=\frac{1}{n_\alpha}\int_{-\infty}^{+\infty}dv_x\int_{-\infty}^{+\infty}dv_y(\mathbf{v}-\mathbf{U}_\alpha)^2 f_\alpha(x,v_x,v_y,t), \tag{7}$$

of each species α.

The Vlasov code [23] has been run in the regime $k_0\lambda_{De}\approx 2$ (λ_{De} is the electron Debye length), for several wave angular frequencies ω_0 (normalized over ω_{pi}) in the range 1.7–2.12, where $\omega_0=4\omega_{ci}\approx 1.93$, and for several values of the normalized peak field amplitude, from $a=10^{-4}$ to 5×10^{-3} (corresponding to the electric field in the range 5–200 kV/cm). A hydrogen plasma ($A=Z=1$) is considered throughout the present paper.

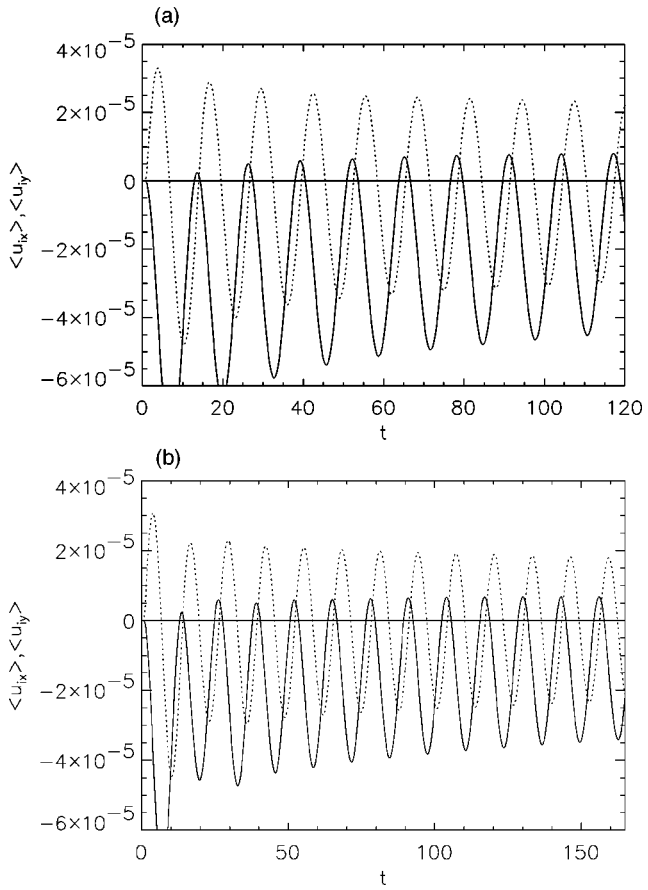

FIG. 2. $\langle U_{iy}\rangle$ (solid lines) and $\langle U_{ix}\rangle$ (dotted lines) are plotted versus time, for $\omega_0=1.93$ (a), and for $\omega_0=1.7$ (b).

When the pump wave is switched on, after few ion cyclotron periods, a stationary state is established, in which the ions oscillate around an average negative U_{iy} while the electron oscillations do not manifest any specific transverse drift velocity. These behaviors are preserved even after performing a spatial average of $U_{\alpha y}$ over the entire x range of integration. In Fig. 1, the electron U_{ey} fluid velocity (solid line) is displayed as a function of time at $x=0.038$, for $\omega=1.93$, and $a=10^{-3}$. Since on the typical electron time scales the applied field oscillates very slowly, we expect that electrons will execute slow drift oscillations in the y direction, superimposed to their fast Larmor rotation. Qualitatively, it is just what is observed in Fig. 1, where the normalized drift velocity $v_{ed}=-E_x/B_z$ is also plotted (dashed lines) superimposed to the instantaneous y component of the electron fluid velocity U_{ey}. Here, the drift velocity has been computed using the electric field which is solution of the Poisson equation, Eq. (2), and the magnetic field which is the sum of that initially applied (the dominant one) plus the small component which is generated during the interaction. The different amplitudes between the two curves can be ascribed mainly to the convective term in the fluid equation of motion, that is, to the nonlinearity of the electron dynamics.

The average nonzero ion drift velocity in the y direction, $\langle U_{iy}\rangle$, is clearly visible in Fig. 2, where it is plotted (full lines) for $\omega_0=1.93$ (a) and for $\omega_0=1.7$ (b) (far from $4\omega_{ci}$ and from any cyclotron subharmonics). The spatial average

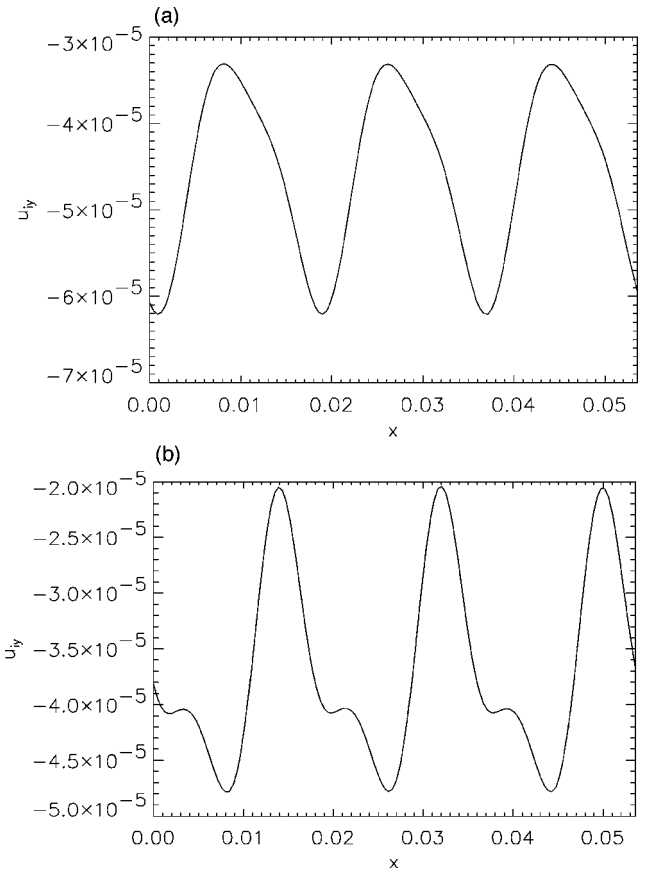

FIG. 3. U_{iy} is shown for $\omega_0=1.93$ (a) and $\omega_0=1.7$ (b) at $t=60$.

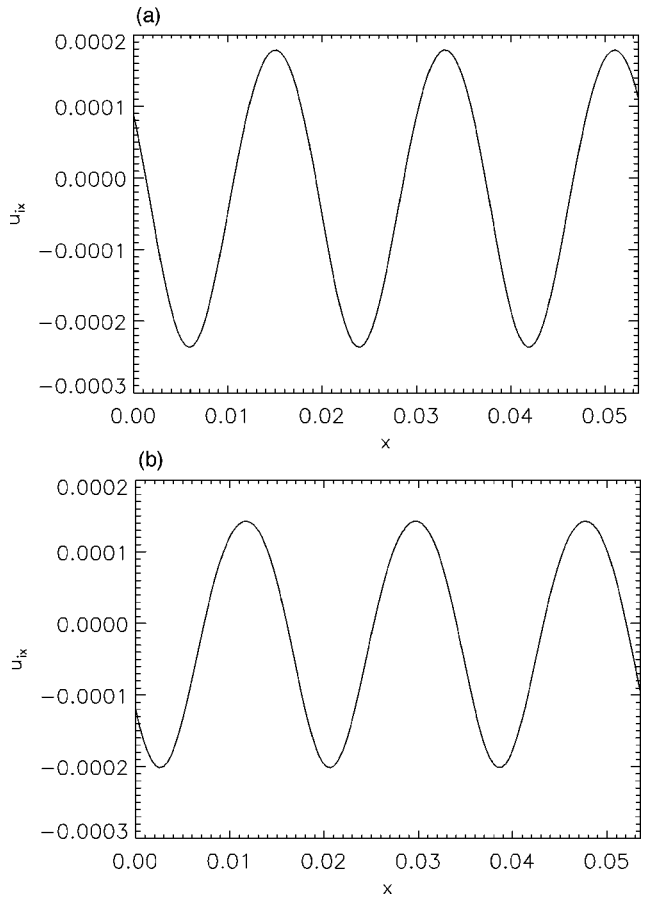

FIG. 4. U_{ix} is shown for $\omega_0=1.93$ (a) and $\omega_0=1.7$ (b) at $t=60$.

of U_{iy} leaves visible only the fluid oscillations at ω_{ci} (the oscillations at the pump frequency are averaged out), which at the end of the integration reach a quasistationary state, where the center of the oscillation is shifted towards negative values. On the same plot, the x component of the ion fluid velocity is also shown (dotted lines), which does not manifest any appreciable drift.

The oscillations on the moments of first order of the ion distribution function are due to its nonequilibrium character acquired under the action of the pump wave. Moreover, we expect that the ion distribution function is asymmetrically distorted in the U_{iy} direction. We shall discuss the kinetic aspects of the interaction in the following section.

The spatial dependence of the ion fluid velocity U_{iy} is shown in Fig. 3 at $t=60$ for $\omega_0=1.93$ (a) and for $\omega_0=1.7$ (b). It is seen that in both the cases, the response of the plasma contains harmonics which are nonlinearly generated during the interaction. On the other hand, no harmonic content appears in the x component of the macroscopic ion velocity as is seen in Fig. 4. In addition, plots of the ion plasma density (which we do not display here) show regular oscillations at $\omega=\omega_{ci}$ in time and at $k=k_0$ in space, of peak amplitude $\pm5\%$.

In Fig. 5, the ion energy content, as defined by Eq. (7), is plotted versus time for $a=10^{-3}$ and several pump frequencies: $\omega_0=1.93$ (full line), and $\omega_0=1.9$ (dotted line), $\omega_0=1.7$ (dashed line). The ion temperature is averaged over the spatial integration range. It is seen that ions are slowly ''heated'' during the interaction with the wave depending on the interaction conditions. Here, the ion temperature is normalized over m_ic^2. Electrons are also heated due to the nonlinear excitation of high frequency plasma modes. In order to understand the basic mechanism leading to electron heating, let us consider the frequency spectrum of the longitudinal

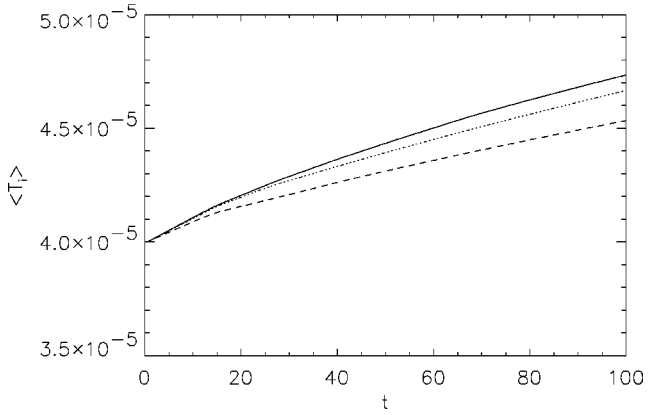

FIG. 5. $\langle T_i\rangle$ (normalized over m_ic^2 and averaged over the space) is plotted versus time for $a=10^{-3}$ and several pump frequencies: $\omega_0=1.93$ (full line), $\omega_0=1.9$ (dotted line), and $\omega_0=1.7$ (dashed line).

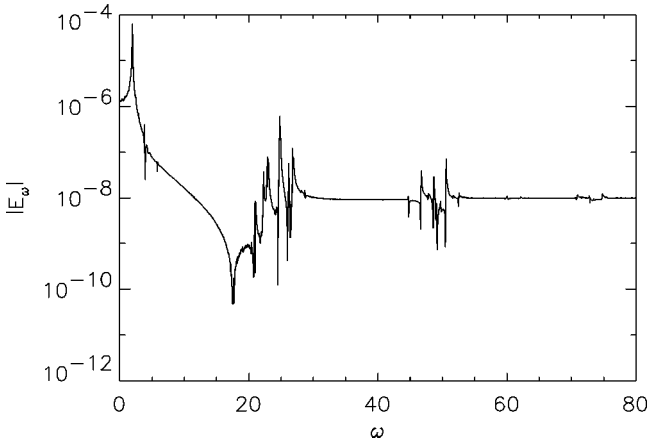

FIG. 6. $|E_\omega|$ is plotted versus ω at $x=0$ for $\omega_0=1.93$ and $a=10^{-3}$.

electric field. $|E_\omega|$ versus ω is plotted in Fig. 6, at $x=0$, for $\omega_0=1.93$ and $a=10^{-3}$. In the low frequency range, we have peaks at the pump ω_0 and at its second harmonic $2\omega_0$. In the high frequency interval, two main peaks at $\omega_{ce}\approx\omega_{uh}$ and at $2\omega_{ce}$ occur accompanied by sidebands which differ by $\pm\omega_0$ and $\pm 2\omega_0$. It means that a broad spectrum of electric field fluctuations, at frequencies higher than ω_0, acting on the plasma, that is preferentially on the electrons, is produced during the interaction. The high frequency oscillations are a consequence of the different mobility of electrons and ions perpendicularly to the external magnetic field. Charge separations are induced by the low frequency pump field and the electrons respond on their characteristic time scales.

The transverse component of the ion fluid velocity, averaged over the spatial range of integration, $\langle U_{iy}\rangle$, has been computed for different values of the angular frequencies ω_0 of the pump wave in the range 1.7–2.12 and several values of the normalized peak field amplitude in the range $a\in[10^{-4};5\times10^{-3}]$. For most of the considered cases, the ordered ion dynamics reaches a quasistationary state over

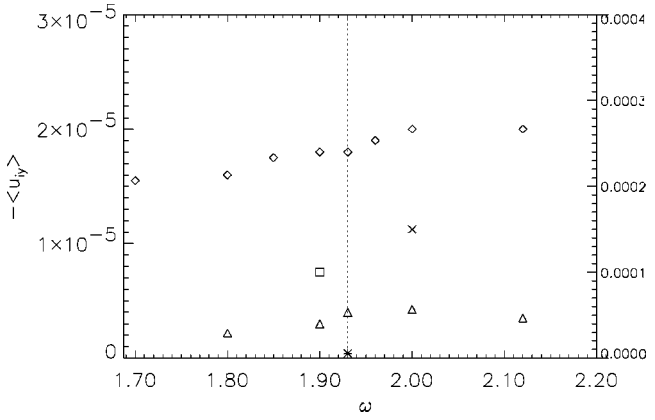

FIG. 7. $\langle U_{iy}\rangle$ is plotted versus ω_0, for $a=10^{-4}$ (*), 3×10^{-4} ($\triangle$), 10^{-3} ($\diamond$), 3×10^{-3} ($\square$), 5×10^{-3} ($\times$). The left-hand-side vertical axis refers to the cases $a=10^{-4}$,3×10^{-4}, and 10^{-3}. The right-hand-side axis refers to the cases $a=3\times10^{-3}$, and 5×10^{-3}. The vertical dotted line indicates $\omega_0=4\omega_{ci}$.

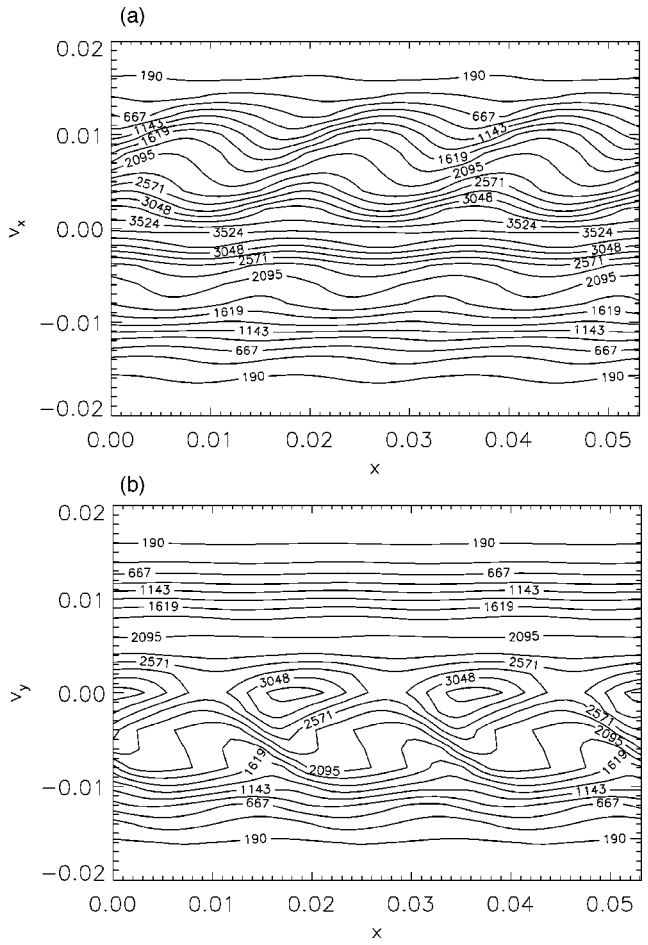

FIG. 8. The contour lines of $f_i(x,v_x,v_y0)$ (a) and of $f_i(x,v_x=0,v_y)$ (b) are shown at $t=52$ for $\omega_0=1.93$ and $a=10^{-3}$.

100–120 times, in unit of ω_{pi}^{-1}, although the electron "temperature" may still increase. In Fig. 7 $\langle U_{iy}\rangle$ is plotted versus the pump frequency, for several values of the wave amplitude: $a=10^{-4}$ (*), 3×10^{-4} ($\triangle$), 10^{-3} ($\diamond$), 3×10^{-3} ($\square$), 5×10^{-3} ($\times$). The left-hand-side vertical axis refers to the cases $a=10^{-4}$, 3×10^{-4}, and 10^{-3}. The right-hand-side axis refers to the cases $a=3\times10^{-3}$ and 5×10^{-3}. We observe that (i) the ion drift velocity is always present and that it is definite negative; (ii) no particular ion response occurs around the frequency $\omega_0=4\omega_{ci}$; (iii) the amplitude of the ion drift increases monotonously with the pump amplitude. Average ion velocities in the range 1–10 km/s have been found, which are comparable with those predicted by previous analyses [16].

IV. THE EVOLUTION OF THE PARTICLE DISTRIBUTION FUNCTIONS

In this section, we examine the time evolution of the distribution functions of the ions and of the electrons under the action of the pump wave described in Sec. II. We begin by considering the ion phase spaces (x,v_x) and (x,v_y). In Fig. 8, the contour lines of (a) $f_i(x,v_x,v_y=0)$ and of (b) $f_i(x,v_x=0,v_y)$ are shown at $t=52$, for $\omega_0=1.93$ and

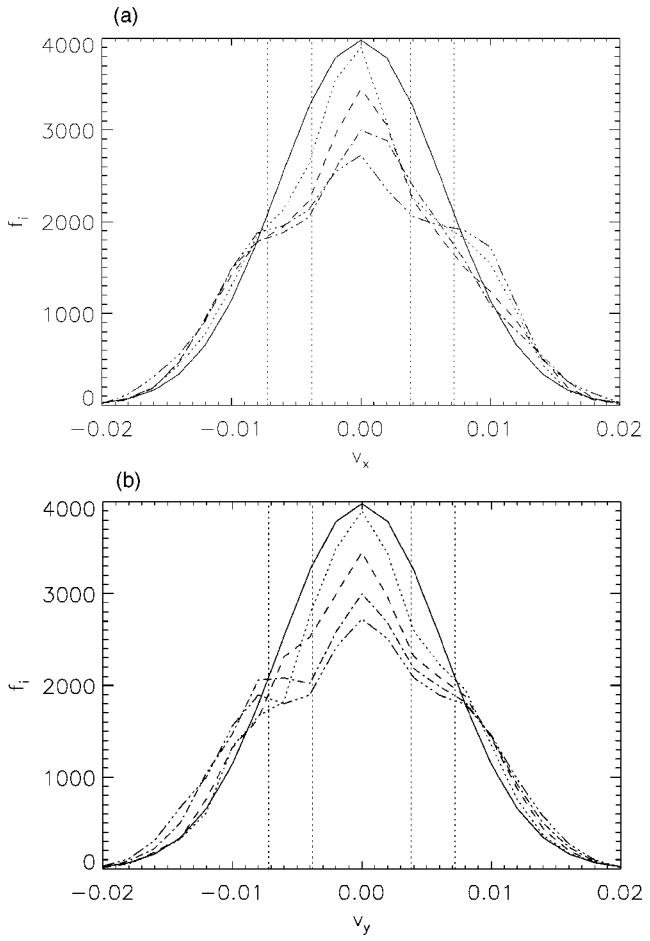

FIG. 9. The ion distribution fucntion $f_i(x,v_x,v_y)$ is plotted (a) versus v_x at $x=0.026$ and $v_y=0$ and (b) versus v_y, at the same spatial position and $v_x=0$, for the same parameters as in Fig. 8. The five curves refer to different times, namely, $t=0$ (solid line), 32 (dotted line), 64 (dashed line), 96 (dot-dashed line), 124 (triple dot-dashed line). The vertical dotted lines indicate the resonant velocity ranges where ion trapping is expected in an unmagnetized plasma, according to the discussion in Sec. V.

$a=10^{-3}$. These plots well represent what happens all along the wave-plasma interaction: that is, (i) in the v_x direction , the ion distribution function flattens, more clearly at $v_x>0$, and (ii) in the v_y direction, the ion distribution develops a kind of vortices in the $v_y<0$ side.

In Fig. 9, the ion distribution function is plotted (a) versus v_x, at $x=0.026$ and for $v_y=0$, and (b) versus v_y, at the same spatial position and for $v_x=0$, for the same parameters as in Fig. 8. The five curves refer to different times, namely, $t=0$ (solid line), 32 (dotted line), 64 (dashed line), 96 (dot-dashed line), and 124 (triple dot-dashed line). By inspection of Figs. 8 and 9, we can notice that the distribution function is distorted and develops a sort of *plateau* in the ranges $|v_x|,|v_y|\approx 0.003$–0.008 (up to 0.01 for positive v_x); at later times, it manifests even a population inversion for negative v_y's. In general, we observe that the main effect of the interaction with the wave is localized within this ''special'' velocity interval. Notice that the phase velocity of the pump wave, $\omega_0/k_0\approx 0.0055$ lies well within this range. It is the manifestation of the *transverse ion Landau damping* and of the related ion trapping which accompany the interaction between the wave and the ion population. The features of this trapping process are those of unmagnetized charged particles and their occurrence in magnetized plasmas has been discussed in Refs. [24,25]. Strictly speaking, for very high frequencies, i.e., $\omega_0 \gg \omega_{ci}$, the wave interaction can be treated as the ions were unmagnetized over few wave cycles only. Over longer times, it is expected that the proper features of the magnetized ions would become dominant. However, we should stress that in our simulations, the transverse Cherenkov resonance persists over times much longer than the ion Larmor period. Indeed, in our case, $\omega_0 \approx 4\omega_{ci}$ turns out to be large enough to make the interaction of this type for the whole integration time, corresponding to about ten ion cyclotron periods. It is worth noticing that the effect of the presence of the magnetic field is to transfer the trapping process from the v_x direction ($\mathbf{k}_0$ has the x component only) to the v_y-direction. The vertical dotted lines in Fig. 9 indicate the resonant velocity ranges where ion trapping is expected in an unmagnetized plasma, according to the discussion in Sec. V. For the sake of completeness, we wish to remind that from a quasilinear point of view, since $k_{||}=0$ and no relativistic dependence of the ion mass on the ion velocity is considered, the well known linear resonant condition reads $\omega=n\omega_{ci}$ (n being a positive integer), and strictly speaking, no resonant velocity exists [26].

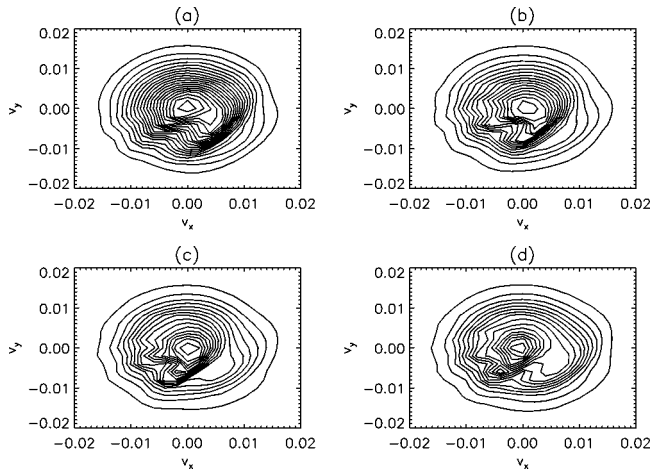

FIG. 10. The level lines of $f_i(v_x,v_y)$ are shown at $x=0.026$ for $t=4$ (a), $t=8$ (b), $t=12$ (c), and $t=16$ (d).

The time evolution of the ion distribution function under the action of the pump wave is shown in Fig. 10, where the level lines of $f_i(v_x,v_y)$ are shown at $x=0.026$, for $t=4$ (a), $t=8$ (b), $t=12$ (c), and $t=16$ (d). As it is evident by the sequence, the initially isotropic distribution is affected by the wave, manifesting a modulation of the contours in the half plane $v_y<0$. The ''tips'' on the contours appear as bumps of the ion distribution on the right-hand side of each plot, around the point $v_x=0.006$–0.007, $v_y=-0.007$. Then they ''rotate'' clockwise, disappearing when they reach the left-hand side of the plot; at the same time new tips appear for

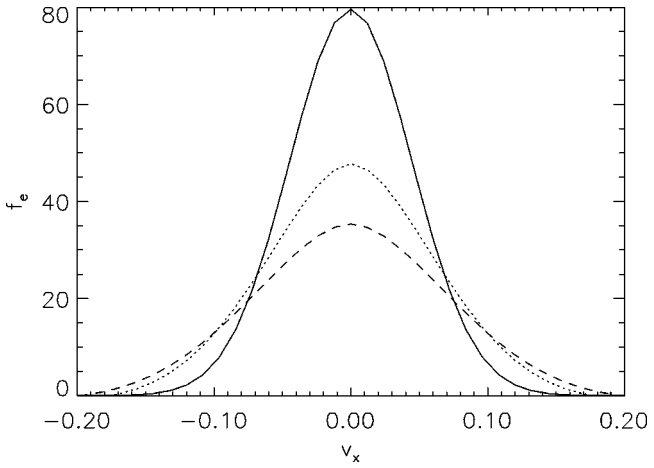

FIG. 11. The electron distribution function $f_e(x,v_x,v_y)$ is plotted versus v_x for $v_y=0$ and x corresponding to the center of the simulation box at $t=0$ (full line), $t=64$ (dotted line), and $t=128$ (dashed line).

positive v_x values, rotating to the left, and disappearing for negative v_x values. In other words, the pump wave couples with resonant ions with $v_x \approx \omega_0/k_0$, flattening the distribution along v_x. Then the Larmor rotation of the ions brings this perturbation in the half plane $v_y<0$. Going from $v_y<0$ to $v_y>0$ the distribution function relaxes, resulting in the net effect of the wave-plasma interaction mainly localized at negative v_y values. These perturbations of the ion distribution function are at the origin of the transverse ion drift.

The electron distribution function behaves much more smoothly. As it is seen from Fig. 11, its shape remains Gaussian-like even if it is broadened. As we mentioned in Sec. III, the electrons see the pump as an almost uniform and slowly oscillating electric field. In addition, electrons are also acted upon by the discrete frequency spectrum localized around the electron cyclotron frequency (see Fig. 6), which is at the origin of the electron heating.

V. DISCUSSION OF THE RESULTS

The kinetic analysis which has been presented in this paper shows that the nonlinear character of the interaction of a finite amplitude electrostatic wave propagating at 90° with respect to an externally imposed magnetic field leads to the generation of a transverse drift ion velocity of definite sign. This effect cannot be explained in the frame of a linear theory. The simplest physical mechanism which can be invoked to explain the appearance of a transverse (to both $\mathbf{k}_0$ and $\mathbf{B}_0$) ion drift is the momentum transfer from the propagating wave to the resonant ions. Notice that according to our analysis, the resonant ions are those undergoing the transverse Landau damping, that is, satisfying the relationship $v_x \approx \omega_0/k_0$. If a photon associated with an IBW, with momentum $\hbar\mathbf{k}_0=\hbar k_0\hat{\mathbf{e}}_x$, is absorbed by a resonant ion spiralling around the magnetic field, the x component of the ion momentum, p_x, increases to $p_x'=p_x+\hbar k_0$. Here, $\hat{\mathbf{e}}_x$ represents the unitary vector in the x direction. Then the ion orbit is modified in such a way that its Larmor radius increases (decreases) at larger (smaller) x displacement from its center of gyration, leading to an overall average ion drift in the negative y direction (the same result has been found in Ref. [16] on the basis of an approximated single-particle analysis). In the above picture, it is assumed that the ion gains the momentum $\hbar\mathbf{k}_0$ before completing a Larmor orbit (almost instantaneously). From a macroscopic point of view, this effect can be interpreted as due to a force $\mathbf{F}_w$ (of the second order in the wave amplitude), exerted by the IBWs on the resonant (and, therefore, absorbing) ions and due to the spatial variations of the intensity of the incoming electrostatic wave. An $\mathbf{F}_w\times\mathbf{B}_0$ ion drift then arises which in the geometry that we have considered is directed as $-\hat{\mathbf{e}}_y$. We observe that the basic nonlinearity due to the deformation (anisotropy) of the ion trajectory with respect to the (isotropic) circular one poses an obstacle to the use of the standard quasilinear theory to investigate the process of transverse flow generation, since this approach assumes the complete isotropy of the unperturbed particle orbit around the magnetic field [26]. In addition, the fact that the wavelength is of the same order of or smaller than the ion Larmor radius is a necessary condition, to the flow generation since under such conditions the ions ''see'' a propagating wave, instead of a dipole field as if $\lambda_0 \gg \rho_{Li}$.

One important result of our investigation is that during the wave-plasma interaction, the ion distribution function becomes strongly distorted preferentially in a velocity range which looks directly correlated to the wave phase velocity, thus showing that the momentum transfer from the wave to the ions occurs via a transverse Cherenkov resonance. The process of perpendicular Landau damping and the consequent ion trapping at the wave phase velocity in the presence of a magnetic field have been described in Refs. [24,25], and later in Ref. [27], on the basis of a single-particle analysis. In the early papers, the nonlinear behavior of an ion under the action of a lower hybrid wave, in the presence of a uniform magnetic field, has been investigated by studying the particle trajectories. The objective of the work, and of successive papers [10–12], was to assess the heating efficiency of electrostatic waves beyond the linear approximation, retaining particle trapping effects and exploiting the stochasticity of the ion motion.

The main idea is that, when a magnetized charged particle is acted upon by a finite-amplitude longitudinal wave, its orbit is distorted in a nontrivial way by the applied electric field. Its effect emerges more evident when the pump amplitude is finite and its wavelength is of the same order of or smaller than the particle Larmor radius. Over a single Larmor orbit, if the wave frequency is appreciably larger than the cyclotron frequency, Landau damping and the consequent trapping occurs since pieces of the ion trajectories can be approximated by straight segments, that is ions behave as unmagnetized. Following Ref. [25] we calculate the lower and upper boundaries of the trapping region in the velocity space. From the inequality $|v-\omega_0/k_0|<\sqrt{(a/k_0)}$ (in normal-

ized units), we find that trapping would occur in the range $3.8\times10^{-3}<v<7.2\times10^{-3}$, which turns out to be a good estimate of the location and of the extension of the *plateau* in Fig. 9. Moreover, the estimate of the maximum ion heating during one Larmor period [25] as $2(\omega_0/k_0)(a/k_0)^{1/2}\approx2\times10^{-5}$, well fits with the corresponding value taken from Fig. 5. An important point is that the numerical integrations we have performed show that this regime of interaction is not limited to the first Larmor period, but extends at least over ten cyclotron orbits, after which a quasistationary state is achieved.

Observe that some of the consequences of the actual orbit shape can be hidden if a gyrophase average is performed over the particle trajectory, as it is the case when the standard quasilinear theory is developed. Under such conditions, transverse average particle motions (such as the transverse drift discussed in this paper) are canceled out.

Finally, our model assumes the spatial uniformity of the background plasma as well as of the pump amplitude. In a real experiment, the wave intensity is absorbed during its propagation and its spatial distribution (in the x direction in our model, and in the radial direction in the tokamak geometry) develops an inhomogeneity. In this case, the resulting gradient of the IBW intensity when crossing the absorbing plasma region is also at the origin of a (ponderomotive) force $\mathbf{F}_{pm}\propto-\nabla E^2\|\hat{\mathbf{e}}_x$, which also is expected to drive a transverse ion drift along $-\hat{\mathbf{e}}_y$.

VI. SUMMARY AND OPEN QUESTIONS

The generation of a coherent ion flow due to the injection of a purely electrostatic wave of finite amplitude propagating at right angle with the externally imposed uniform magnetic field has been investigated by means of a kinetic code which solves the fully nonlinear Vlasov equations for electrons and ions, coupled with the Maxwell equations, in one spatial and two velocity dimensions. A uniformly magnetized plasma slab has been considered. The wave frequency has been chosen in the range of the fourth ion cyclotron harmonic, and the wavelength of the order of the thermal ion Larmor radius in order to model the propagation of an ion Bernstein wave.

The principal results of this work can be summarized in the following points:

(i) A quasistationary transverse (to both the magnetic field and pump wave vector) average ion drift velocity is produced quite independent of the pump frequency and amplitude.

(ii) Over more than ten-ion cyclotron periods (the full time interval of our integrations, at which a quasistationary state is achieved), the wave-plasma interaction manifests the features of the particle trapping, characteristic of the ion transverse Landau damping, in the velocity range of the wave phase velocity, the width of which turns out to be well described by the formula $\Delta v\approx2\sqrt{eE_0/m_ik_0}$. It can be considered as a remnant of the particle trapping in a slightly magnetized plasma (with $\omega_0\gg\omega_{ci}$) when the wave absorption occurs before a full ion Larmor orbit is completed. In the debate about the ''Bernstein-Landau paradox'' [14,15], our results show that although we have only $\omega_0\approx4\omega_{ci}$, the transverse Landau damping is the dominant mechanism of wave-plasma coupling, which leads to the effective plasma heating and momentum generation. Our results have important implications on the correct way of determining the rate of energy and momentum transfer from the pump wave to the plasma, as well as the spatial localization of the interaction, as can be easily realized if we think that the well established quasilinear theory for magnetized plasmas does not predict the existence of resonant particles for pure perpendicular propagation (since we are treating keV ions, we ignore the relativistic mass dependence on the particle velocity).

(iii) Such an interaction produces *plateau* regions in the ion distribution functions in both v_x and v_y directions, but in an asymmetric way: population inversion occurs only for negative v_y's, which is at the basis of the apperance of the transverse ion flow along the negative y axis.

(iv) The nonlinear spectral broadening both in the frequency and wave vector domains predicted by the full Vlasov approach enriches the physical picture of the wave-plasma interaction. In particular, electrons turn out to be heated due to the nonlinear generation of spectral structures around the electron cyclotron frequency and its second harmonic, while the electron distribution function remains Gaussian-like.

This scenario gives rise to basic questions which deserve further analysis. First, the present investigation has been made with a reduced ion-to-electron mass ratio. The extension of the presented physical picture of the wave-plasma interaction to the case with $\Lambda_e=1836$ needs to be worked out, and it is the matter of the present study. Indeed, the ion-to-electron mass ratio plays an important role in the linear theory of the IBW propagation, in that the dispersion changes depending on whether the lower hybrid resonance is smaller or larger than the considered cyclotron harmonic. The reduced ion mass makes $4\omega_{ci}>\omega_{lh}$, while for the actual proton mass $4\omega_{ci}<\omega_{lh}$. However, the collisionless absorption mechanism predicted by the linear theory depends on how close to a cyclotron harmonic the wave frequency is, and that is exactly the aspect of the wave-plasma interaction we have investigated. Therefore, we do not expect that the use of the reduced ion mass affects the qualitative description of the wave-plasma coupling physics. Second, the wave propogation at a finite angle with the normal to the magnetic field should be considered. This introduces the ion cyclotron damping which is lost at strictly perpendicular propagation. To this objective, two extra dimensions, one spatial (z) and one in velocity (v_z), should be considered in the code. However, this would require a much larger storage memory for tha data during the computation. Third, spatial gradients should be allowed for, in order to simulate the actual wave propagation in a confined plasma. This aspect of the problem can be studied to a certain extent with a periodic boundary condition code. However, nonperiodic boundary conditions would allow a more realistic description of the power deposition of the excited IBW in a nonuniform plasma.

The model used here, although too simplified for a direct comparison with the experimental results, has allowed us to investigate the basic kinetic aspects of the interaction of an

externally driven, purely electrostatic wave with a magnetized electron-ion plasma. Since the full analysis of an electron-ion plasma, which must resolve both the electron and the ion time and spatial scales, is extremely time consuming, the results presented here, although for a reduced ion mass, are a necessary step towards the implementation of simplified models (as, for example, a massless electron model) which allow one to use the correct parameter values. Indeed, a massless electron model, with the physical correct ion mass value, is under development starting from the results presented in this paper.

ACKNOWLEDGMENTS

The authors wish to acknowledge useful discussions and suggestions by S.V. Bulanov, A. Cardinali, C. Castaldo, D. Farina, N. Fisch, C. Karney, E. Lazzaro, A. Mangeney, R. Pozzoli, and F. Valentini. Part of this work was supported by the INFM Parallel Computing Initiative.

[1] G.G. Craddock, P.H. Diamond, M. Ono, and H. Biglari, Phys. Plasmas **1**, 1944 (1994).
[2] L.A. Berry, E.F. Jaeger, and D.B. Batchelor, Phys. Rev. Lett. **82**, 1871 (1999).
[3] E.F. Jaeger, L.A. Berry, and D.B. Batchelor, Phys. Plasmas **7**, 641 (2000).
[4] E.F. Jaeger, L.A. Berry, and D.B. Batchelor, Phys. Plasmas **7**, 3319 (2000).
[5] R. Cesario *et al.*, Phys. Plasmas **8**, 4721 (2001).
[6] Z. Lin, T.S. Hahm, W.W. Tang, and R.B. White, Science **281**, 1835 (1998).
[7] J.R. Wilson *et al.*, Phys. Plasmas **5**, 1721 (1998).
[8] B.P. LeBlanc *et al.*, Phys. Rev. Lett. **82**, 331 (1999).
[9] Y. Bao *et al.*, in *Proceedings of the 28th European Physical Society Conference on Controlled Fusion and Plasma Physics, Funchal, 2001*, edited by C. Silva, C. Varander, and D. Campbell (European Physical Society, Lisboa, 2001), pp. 1177–1180.
[10] C.F. Karney and A. Bers, Phys. Rev. Lett. **39**, 550 (1977).
[11] C.F.F. Karney, in *Intrinsic Stochasticity in Plasmas*, edited by G. Laval and D. Gresillon (Editions de Physique, Orsay, 1979), p. 159.
[12] C.F.F. Karney, Phys. Fluids **21**, 1584 (1978); **22**, 2188 (1979).
[13] A.J. Lichtenberg and M.A. Lieberman, *Regular and Stochastic Motion* (Springer, New York, 1983).
[14] G.M. Zaslavskii, M.A. Malk'ov, R.Z. Sagdeev, and V.D. Shapiro, Sov. J. Plasma Phys. **12**, 453 (1986).
[15] A.I. Sukhorukov and P. Stubbe, Phys. Plasmas **4**, 2497 (1997).
[16] A. Cardinali, C. Castaldo, and R. Cesario, in *Joint Varenna-Lausanne International Workshop on Theory of Fusion Plasmas*, edited by E. Sindoni, F. Troyon, and J. Vaclavik (Editrice Compositori, Bologna, 1998), p. 519.
[17] M. Lontano and F. Califano, in *Joint Varenna-Lausanne International Workshop on Theory of Fusion Plasmas*, edited by J.W. Connor, O. Sauter, and E. Sindoni (Editrice Compositori, Bologna, 2000), p. 267.
[18] C. Marchetto, F. Califano, and M. Lontano, in *Proceedings of the 28th European Phyiscal Society Conference on Controlled Fusion and Plasma Physics, Funchal, 2001*, edited by C. Silva, C. Varander, and D. Campbell (European Physical Society, Lisboa, 2001), pp. 1133–1136.
[19] F. Califano and M. Lontano, Phys. Rev. E **58**, 6503 (1998).
[20] F. Califano and M. Lontano, Phys. Rev. Lett. **83**, 96 (1999).
[21] M. Lontano and F. Califano, Phys. Rev. E **61**, 4336 (2000).
[22] R. Cesario, *et al.*, in *Radio Frequency Power in Plasmas*, edited by Stefano Bernabei and Franco Paoletti, AIP Conf. Proc. No. 485 (AIP, Melville, 1999), p. 100.
[23] A. Mangeney, F. Califano, C. Cavazzoni, and P. Travnicek, J. Comput. Phys. **179**, 495 (2002).
[24] C.F. Kennel and F. Engelmann, Phys. Fluids **9**, 2377 (1966), see Eq. (2.16), and the discussion thereafter.
[25] A. Fukuyama, H. Momota, R. Itatani, and T. Takizuka, Phys. Rev. Lett. **38**, 701 (1977).
[26] C.F.F. Karney, Ph.D. thesis, Massachusetts Institute of Technology, 1977 (unpublished).
[27] M. Brambilla, *Kinetic Theory of Plasma Waves* (Clarendon, Oxford, 1998), Secs. 31 and 40.